



## Optimization of corner micro end milling by finite element modelling for machining thin features

Davoudinejad, Ali; Li, Dongya; Zhang, Yang; Tosello, Guido

*Published in:*  
Procedia CIRP

*Link to article, DOI:*  
[10.1016/j.procir.2019.04.158](https://doi.org/10.1016/j.procir.2019.04.158)

*Publication date:*  
2019

*Document Version*  
Publisher's PDF, also known as Version of record

[Link back to DTU Orbit](#)

*Citation (APA):*  
Davoudinejad, A., Li, D., Zhang, Y., & Tosello, G. (2019). Optimization of corner micro end milling by finite element modelling for machining thin features. *Procedia CIRP*, 82, 362-367.  
<https://doi.org/10.1016/j.procir.2019.04.158>

---

### General rights

Copyright and moral rights for the publications made accessible in the public portal are retained by the authors and/or other copyright owners and it is a condition of accessing publications that users recognise and abide by the legal requirements associated with these rights.

- Users may download and print one copy of any publication from the public portal for the purpose of private study or research.
- You may not further distribute the material or use it for any profit-making activity or commercial gain
- You may freely distribute the URL identifying the publication in the public portal

If you believe that this document breaches copyright please contact us providing details, and we will remove access to the work immediately and investigate your claim.

## 17th CIRP Conference on Modelling of Machining Operations

## Optimization of corner micro end milling by finite element modelling for machining thin features

Ali Davoudinejad\*, Dongya Li, Yang Zhang, Guido Tosello

*Department of Mechanical Engineering, Technical University of Denmark, Building 427 A, Produktionstorvet, 2800 Kgs. Lyngby, Denmark*\* Corresponding author. Tel.: +45-45254897; fax: +0-000-000-0000. E-mail address: [alidav@mek.dtu.dk](mailto:alidav@mek.dtu.dk)**Abstract**

Manufacturing thin metal features at miniature scale with high precision milling represents some challenges for different applications such as micro moulds, micro channels, micro gears, surgical instruments, etc. In order to enhance the cutting mechanism understanding and optimize the machining of thin features, 3D finite element modeling (FEM) is applied for the micro end-milling process of thin features. In this study, FE model was used to investigate the minimum wall thickness machinable in order to optimize the experimental machining and enhance the quality of the machined features. Wall thickness uniformity and burr formation were evaluated to achieve the finest overall feature quality. Finally, the FEM prediction results were compared against the experimental tests.

© 2019 The Authors. Published by Elsevier B.V.

Peer-review under responsibility of the scientific committee of The 17th CIRP Conference on Modelling of Machining Operations

*Keywords: Micromilling; Finite Element Modelling; Corner Milling; Thinwall Machining; Industry 4.0***1. Introduction**

Micro thin features or high aspect ratio (HAR) parts are necessary to fulfill the increasing demand of miniaturization in many industries. There are many methods could be employed to manufacture miniature features in micro scale in different materials with both additive and subtractive manufacturing: Selective Laser Melting (SLM), etching, micro-EDM, Digital Light Processing (DLP) micro milling, *etc.* [1][2][3][4].

Micro milling is a popular method as a low-cost and efficient method for thin wall machining. Micro milling has been studied intensively, by the means of experiments and modeling/simulations [5][6][7]. The defects, such as wall bending and burrs, keeping the micro mill stable during the machining process (to reduce the tool wear and chatter) and the lack of systematic control of feature quality are main challenges in micro milling of thin walls. The defects including burr formation, uneven thickness and poor surface quality of the micro milled thin walls are critical issues in thin wall manufacturing. The micro milling parameters and strategies are the most important factors to control the quality. K Popov *et al.* [8] studied the micro milling strategies to manufacture thin wall

ribs and webs. They stressed that the support by the extra fixtures or the un-machined materials should be considered when designing the tool path and that it is very important to minimize of the cutting edge radius in order to reduce the normal component of the cutting force to the wall. Llano *et al.* [5] investigated high aspect ratio micro milling for optimizing the best machined surface quality, uniformity of the thin wall thickness and burr presence on machining aluminium and brass materials. Z-step strategy with a down milling machining approach applied to achieve the best results.

Other literatures studied FE modelling of thin wall machining with helical end mill in macro scales to investigate physical interaction in the process [7]. Izamshah, *et al.* [9] presented a FE model to predict the distortion or deflection of the HAR features during the end milling process aiming to determine the error compensation in short cycle times of production. Zhang, *et al* [10] built a FEA model to investigate the thermal effect of Ti-6Al-4V thin wall structures by micro milling by taking into account of friction power, shearing power and tool-material shear area. Scippa, *et al.* [11] developed a FEM based model for milling process, to optimize

cutting velocity by considering the effects of fixturing, tooltip dynamics, and material removal, during machining.

The aim of this work is to apply a 3D FE based model of micro end milling operation for predicting the main fundamental variables of industrial interest, such as high aspect ratio machining process. In order to control the various wall thickness behaviour in different cutting conditions. This study explore the cutting conditions prior to experimental tests to obtain the high aspect ratio features in the micro milling range.

#### Nomenclature [unites]

$a_p$	axial depth of cut	[ $\mu\text{m}$ ]
$a_e$	radial depth of cut	[ $\mu\text{m}$ ]
$f_z$	feed per tooth	[ $\mu\text{m tooth/rev}$ ]
$v_c$	Cutting speed	[m/s]
$\sigma$	material flow stress	[MPa]
$\varepsilon$	plastic strain	
$\dot{\varepsilon}$	strain rate	
$\dot{\varepsilon}_0$	reference strain rate	
$T$	material temperature	[ $^{\circ}\text{C}$ ]
$T_m$	melting point	[ $^{\circ}\text{C}$ ]
$T_a$	room temperature	[ $^{\circ}\text{C}$ ]
$A$	yield stress	[MPa]
$B$	pre-exponential factor	[MPa]
$C$	strain rate factor	[MPa]
$n$	work hardening exponent	
$m$	thermal softening exponent	

## 2. Numerical procedure

### 2.1. FE Model

The 3D model for micro end-milling Al6082-T6 alloy was simulated using an explicit time integration method by employing a Lagrangian formulation to perform coupled thermo-mechanical transient analysis (AdvantEdge® by Third Wave Systems). The workpiece was a viscoplastic material and represented by the constitutive material model. The effect of material deformation based on the applied load is calculated for non-recoverable deformation. Fig. 1 shows the micro end mill tool used in the experiment and simulation setup with boundary conditions in red for the thin wall corner milling. The part boundary were fixed in the XY and Z bottom directions and the mill constrained in the Z top direction. The feed was applied in the X direction. The tool was modeled with detailed geometry and the CAD model was used for the FEM analysis. The actual tool specifications were listed in Table 1. The tool was modeled in the context of digital manufacturing by directly using the exact geometry of the micro end mill from its cloud of points. The detail of the tool measurement and modeling with cloud of points can be found in the previous work [12]. In the FE modeling of machining process due to the severe distortion of the mesh, the continuous remeshing is a practical solution to overcome this problem in Lagrangian formulation. The continuous remeshing is able to remove the bulk deformation induced the element distortion [13]. The tool and workpiece

were meshed with four node tetrahedral elements, for a total number of 61879 and 60,916 elements, for corner milling.

Table 1 Specifications of MXH225.

Title	Value
Tool manufacturer	NS Tools®
Code	MXH225
Diameter	0.5mm
Material	$\mu$ grain carbide
Coating	TiAlN
Helix angle	$25^{\circ}$
Number of flutes	2
Relief angle	$8^{\circ}$
Flute length	0.5 mm
Cutting edge radius	$3\pm 1 \mu\text{m}$

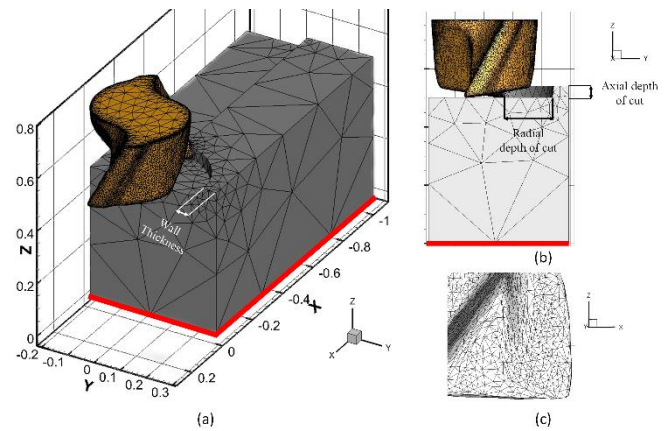


Fig. 1. Workpiece and tool meshing (a) FE model setup; (b) side view; (c) fine mesh region.

### 2.2. Material Model

In order to make a reliable FE model material constitutive behavior is a key issue in the machining conditions. Johnson-Cook (JC) constitutive material model is considered as a trustworthy model (Eq. 1) [14] which was used in many in the previous literatures. Where  $\sigma$  is the material flow stress,  $\varepsilon$  is the plastic strain,  $\dot{\varepsilon}$  is the strain rate,  $\dot{\varepsilon}_0$  is the reference strain rate.  $T$  is the material temperature,  $T_m$  is the melting point and  $T_a$  is the room temperature. The JC constants are as follows:  $A$  is the yield stress,  $B$  is the pre-exponential factor,  $C$  is the strain rate factor,  $n$  is the work hardening exponent and  $m$  is the thermal softening exponent. The thermo-mechanical properties of the workpiece is presented in Table 2 and the material constants used for modelling the plastic behaviour of Al6082-T6 can be seen in Table 3.

$$\sigma = (A + B(\varepsilon)^n) [1 + C \ln(\frac{\dot{\varepsilon}}{\dot{\varepsilon}_0})] [1 - (\frac{T - T_a}{T_m - T_a})^m] \quad (1)$$

Coulomb friction, (Eq. 2) applied in the cutting area. A constant value of friction coefficient used is assigned in this study, as  $\mu = 0.7$ . This value is selected basing on previous experimental identification made by Medaska [15] on Al6061-T6 with carbide tools Al6082-T6 and Al6061-T6 are two

popular aluminum alloys where sometimes replacing each other in the industrial practice due to the similar characteristics.

$$\tau = \mu \sigma_n \quad (2)$$

Table 2 Material properties for Al6082-T6 [16].

Parameter		Value
Young's modulus, (GPa)	E	70
Poisson ratio	$\nu$	0.33
Density (g/cm <sup>3</sup> )	$\rho$	2.70
Thermal conductivity (W/m K)	K	180
Specific heat (J/Kg °C)	Cp	700
Thermal expansion coefficient		24×10 <sup>-6</sup>
Melting temperature (°C)	T <sub>m</sub>	582

Table 3 Coefficients of the JC model for Al6082-T6 [17]

A	B	C	m	n	$\dot{\epsilon}_0$	T <sub>m</sub>	T <sub>a</sub>
(MPa)	(MPa)				(s <sup>-1</sup> )	(°C)	(°C)
214.25	327.7	0.00747	1.31	0.504	1.0	582	21

### 3. Experimental details and machining strategy

In the experiments, the effects of machining strategies have been explored in order to optimize the final quality of the thin walls in the initial phase of the experiments therefore Table 4 presents the final cutting condition employed in the experiments. A five-axis milling machine (MIKRON HSM 400U LP, 5-axis, control unit: Heidenhain iTNC 530 HSCI) were employed to conduct the experiments. The HyperMILL program was used to generate the code. The tool tip geometries were inspected and measured in order to obtain the cutting edge radius and to be compared with CAD model tool.

Table 4 Micro end-milling parameters employed

Parameter	Value
Spindle speed, (rpm)	40000
Feed per tooth (μm tooth/rev)	8
Axial depth of cut (μm)	10, 20, 40
Radial depth of cut (μm)	20
Cutting approach	Down milling

The workpiece was designed in a way to machine three different wall thicknesses 100, 50 and 20 μm with 500 μm height as shown in Fig 2(a) experimental setup. Different machining strategy applied prior to final machining however, better results obtained with the rectangular loop around the wall with down milling approach (Fig. 2(b)). Therefore, the selected depth of cut (10, 20, and 40 μm) was applied for each thickness to evaluate the corner milling process for manufacturing of high aspect ratio features. Fig. 3 shows the experimental results of thin wall top view with 10 μm axial depth of cut. The machining was carried out in dry condition. All the conditions were replicated two time for the consistency of the results. Alicona 3D optical microscope was used for the inspection of the wall quality. The measurement of the wall angle also carried out in the same depth of cut as the initial cut in the simulation to make an equivalent comparison between

experiment and simulated conditions.

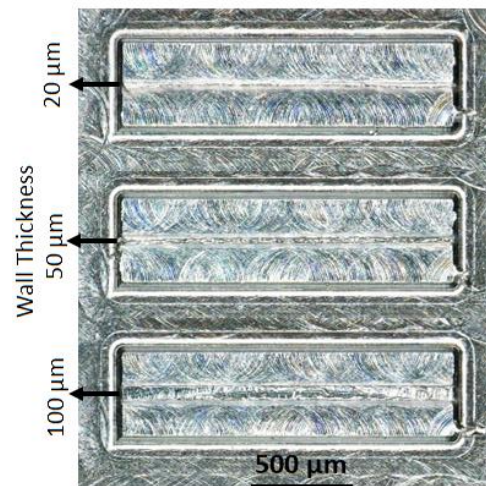
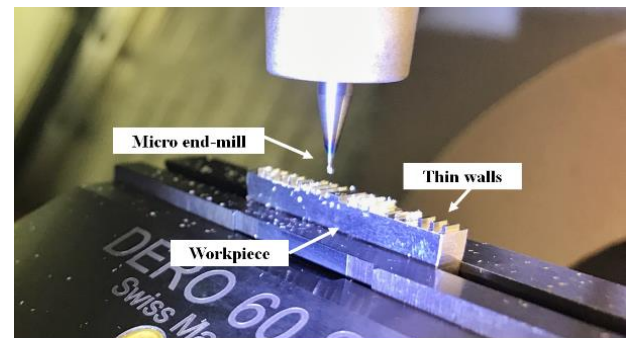
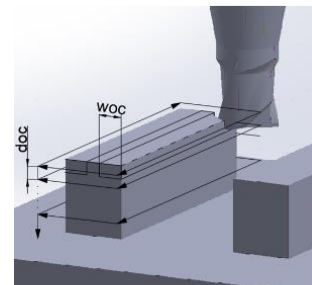


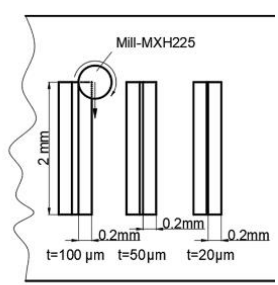
Fig. 2 Machined thin walls of Al6082-T6



(a) Experimental setup



(b) Machining strategy



(c) Wall thickness

Fig. 3 Machining setup and strategy

### 4. Results and discussions,

All the cutting conditions were simulated prior to the experiments and the stresses distribution during machining process was predicted. The thin wall quality was evaluated by inspection of the wall with a 3D microscope. Fig. 4 shows the side view of the stress distribution during micro end milling simulation of thin wall and the experimental machining for three different wall thicknesses and axial depth of cuts. The failure of the wall observed in different cutting conditions. Test 1 to 3 the lowest axial depth of cut (10 μm) was applied and minor deformation was observed in the 20 μm wall in comparison to other conditions with the same thickness. The distortion is more noticeable in the simulations however, in the 50 μm and 100 μm walls the deformation was not detected.



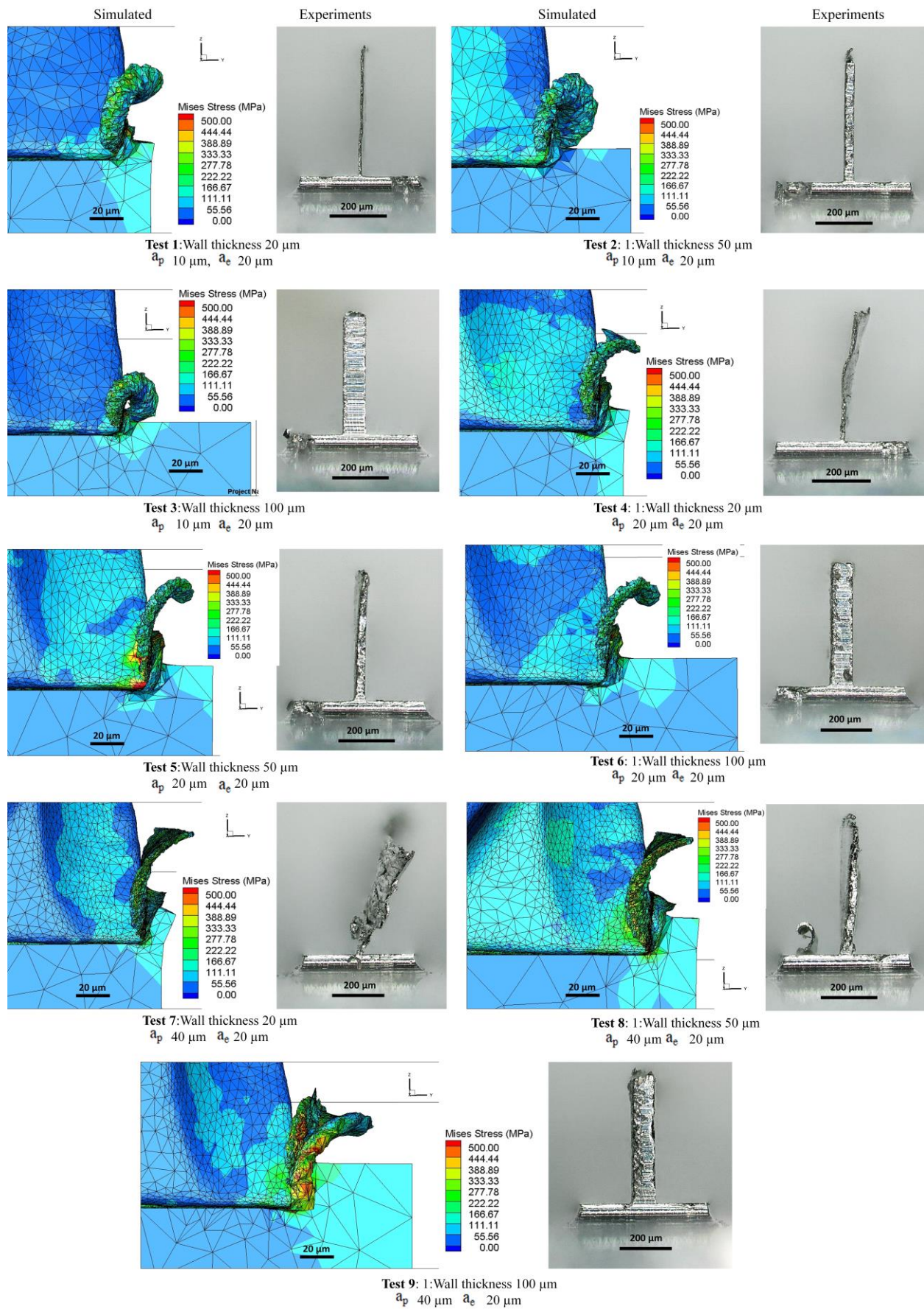


Fig. 4 Von Mises equivalent stress distributions along the thin wall

Respectively, by increasing the axial depth of cut ( $20\text{ }\mu\text{m}$  and  $40\text{ }\mu\text{m}$ ) only  $100\text{ }\mu\text{m}$  wall was not deformed though, in Test 4, 5, 7 and 8 the walls were distorted or warpage occurred along the machined wall. The maximum stress distributed in the wall area was around  $200\text{ MPa}$ , which increased near the cutting zone. The highest stress distribution was observed in a cutting condition with higher axial depth of cut  $40\text{ }\mu\text{m}$  and  $20\text{ }\mu\text{m}$  respectively mainly along the thin wall in the contact region of cutting edge. Fig. 5 illustrate the residual stress distribution in the machined surface at the end of cut (after four teeth engagement  $720^\circ$ ). The maximum stress produced in the wall area was around  $500\text{ MPa}$ , which increased with tool movement in the cutting zone. Furthermore the top and entrance burr formation is visible in the machined area. Fig. 6 shows the comparison between numerical and experimental results of the wall angle, along the tool cutting engagement at the beginning of the cut. The closest value to the nominal angle of the wall was observed with  $a_p=10\text{ }\mu\text{m}$  in  $50$  and  $100\text{ }\mu\text{m}$  wall thickness and  $a_p=20, 40\text{ }\mu\text{m}$  in  $100\text{ }\mu\text{m}$  wall thickness. The maximum error at the top of wall angle was about  $8.5\%$  and most of the conditions were comparable with experimental results with well matching variations trends.

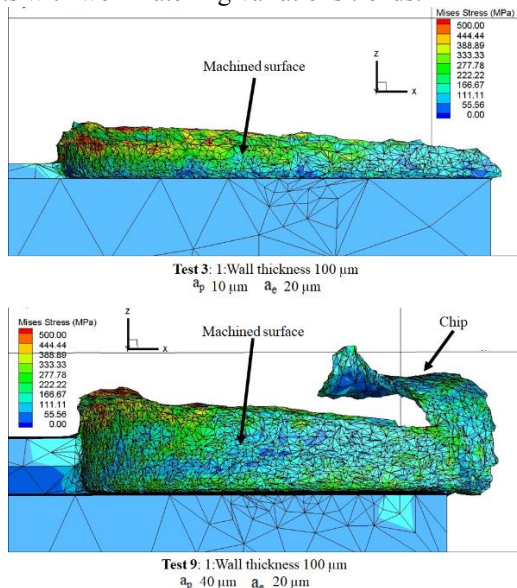


Fig. 5 Stress distribution on the machined surface at the end of cut

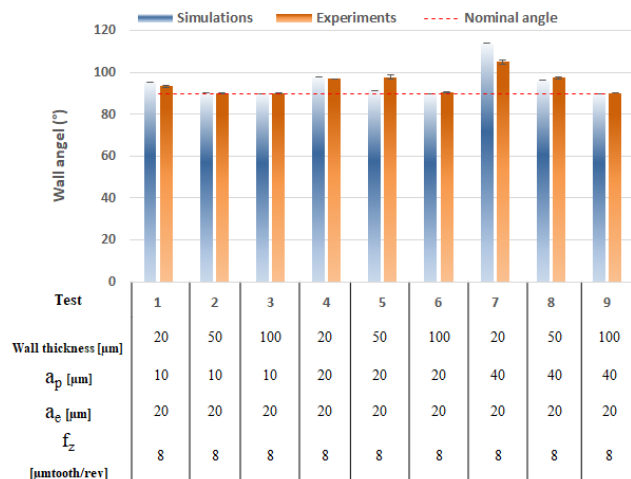


Fig. 6 Comparison of numerical and experimental maximum wall angle

## 5. Conclusion

In this work, a reliable 3D FE model applied to predict the complex process of thin wall micro machining of aluminium alloy. The simulated conditions are verified against experimental tests. The wall quality and uniformity during milling process has been evaluated. In a lower axial depth of cut ( $10$  and  $20\text{ }\mu\text{m}$ ), a better wall condition and a lower wall angle error observed. Concerning the stress distribution along the machined wall larger stress spread in the cutting zone in higher cutting conditions. Regarding wall angle error with cutting conditions a linear trend of deformation recognized in higher condition. A comparable error  $\sim 8.5\%$  at the top of the wall angel between experiment and simulation calculated. This model reduces the basic of costly, and time-consuming initial micro scale experiments for machining high aspect ratio features.

## Acknowledgements

The research leading to these results has received funding from the People Programme (Marie Curie Actions) of the European Union's Seventh Framework Programme (FP7/2007-2013) under REA grant agreement No. 609405 (COFUNDPostdocDTU).

## References

- [1] Song C, Yang Y, Liu Y, Luo Z, Yu JK. Study on manufacturing of W-Cu alloy thin wall parts by selective laser melting. *Int J Adv Manuf Technol* 2015. doi:10.1007/s00170-014-6689-3.
- [2] Liao Y-S, Chen S-T, Lin C-S, Chuang T-J. Fabrication of high aspect ratio microstructure arrays by micro reverse wire-EDM. *J Micromechanics Microengineering* 2005;15:1547–55. doi:10.1088/0960-1317/15/8/024.
- [3] Aimi MF, Rao MP, MacDonald NC, Zuruzi AS, Bothman DP. High-aspect-ratio bulk micromachining of titanium. *Nat Mater* 2004. doi:10.1038/nmat1058.
- [4] Davoudinejad A, Ribo MM, Pedersen DB, Islam A, Tosello G. Direct fabrication of bio-inspired gecko-like geometries with vat polymerization additive manufacturing method. *J Micromechanics Microengineering* 2018;28. doi:10.1088/1361-6439/aabf17.
- [5] Llanos I, Agirre A, Urreta H, Thepsonthi T, Özel T. Micromilling high aspect ratio features using tungsten carbide tools. *Proc Inst Mech Eng Part B J Eng Manuf* 2014. doi:10.1177/0954405414522214.
- [6] Thepsonthi T, Özel T. 3-D finite element process simulation of micro-end milling Ti-6Al-4V titanium alloy: Experimental validations on chip flow and tool wear. *J Mater Process Technol* 2015;221:128–45. doi:10.1016/j.jmatprotec.2015.02.019.
- [7] Bolar G, Joshi SN. Three-dimensional numerical modeling, simulation and experimental validation of milling of a thin-wall component. *Proc Inst Mech Eng Part B J Eng Manuf* 2017. doi:10.1177/0954405416685387.
- [8] Popov K, Dimov S, Pham DT, Ivanov A. Micromilling strategies for machining thin features. *Proc Inst Mech Eng Part C J Mech Eng Sci* 2006. doi:10.1243/09544062JMES192.
- [9] Rai JK, Xirouchakis P. Finite element method based machining simulation environment for analyzing part errors induced during

- milling of thin-walled components. *Int J Mach Tools Manuf* 2008. doi:10.1016/j.ijmachtools.2007.11.004.
- [10] Zhang JF, Ma YH, Feng C, Tang W, Wang S. Thermal modeling and analysis of thin-walled structures in micro milling. *IOP Conf Ser Mater Sci Eng* 2017;265:012017. doi:10.1088/1757-899X/265/1/012017.
- [11] Scippa A, Grossi N, Campatelli G. FEM based cutting velocity selection for thin walled part machining. *Procedia CIRP*, 2014. doi:10.1016/j.procir.2014.03.023.
- [12] Davoudinejad A, Tosello G, Annoni M. Influence of the worn tool affected by built-up edge (BUE) on micro end-milling process performance: A 3D finite element modeling investigation. *Int J Precis Eng Manuf* 2017. doi:10.1007/s12541-017-0157-6.
- [13] D. MT, M. O. Modelling and simulation of high-speed machining. *Int J Numer Methods Eng* n.d.;38:3675–94. doi:10.1002/nme.1620382108.
- [14] Johnson GR, Cook WH. A constitutive model and data for metals subjected to large strains, high strain rates and high temperatures. *7th Int Symp Ballist* 1983:541–7. doi:10.1038/nrm3209.
- [15] Medaska MK, Nowag L, Liang SY. SIMULTANEOUS MEASUREMENT OF THE THERMAL AND TRIBOLOGICAL EFFECTS OF CUTTING FLUID. *Mach Sci Technol* 1999;3:221–37. doi:10.1080/10940349908945691.
- [16] Aalco metals Ltd. Aluminium Alloy 6082 - T6~T651 Plate 2013:24–5.
- [17] Davoudinejad A, Tosello G, Parenti P, Annoni M. 3D finite element simulation of micro end-milling by considering the effect of tool run-out. *Micromachines* 2017;8. doi:10.3390/mi8060187.